Chemosphere 227 (2019) 225–236

Contents lists available at ScienceDirect

Chemosphere

journal homepage: www.elsevier.com/locate/chemosphere

Anthropogenic and lithogenic fluxes of atmospheric lead deposition over the past 3600 years from a peat bog, Changbai Mountains, China

Bobo Guo [a], Jing Wang [b], Chunye Lin [a, *], Mengchang He [a], Wei Ouyang [a]

[a] State Key Joint Laboratory of Environmental Simulation and Pollution Control, School of Environment, Beijing Normal University, Beijing, 100875, China
[b] School of Resource and Environmental Sciences, Wuhan University, Wuhan, 430079, China

HIGHLIGHTS

- We estimate long-term atmospheric Pb deposition flux using ombrotrophic peatlands.
- The effect of human activities, climate change, and volcanic eruptions is analyzed.
- Peat cores in NE China provide long-term records of atmospheric Pb deposition.
- Climate, volcanism, and economic growth influenced anthropogenic Pb concentration.

ARTICLE INFO

Article history:
Received 23 January 2019
Received in revised form
29 March 2019
Accepted 7 April 2019
Available online 8 April 2019

Handling Editor: Martine Leermakers

Keywords:
Lead
Peat bog
Atmospheric deposition flux
Human activity

ABSTRACT

Ombrotrophic peatlands are widely used to reconstruct atmospheric metal deposition histories. Here, we estimated the long-term atmospheric Pb deposition flux using ombrotrophic peatland data from the Changbai Mountains, northeast China. A peat profile of 320-cm depth was sampled and cut into 164 slices for measurement of Pb and other elements by ICP-MS and ICP-AES and radiometric dating by ^{210}Pb, ^{137}Cs and ^{14}C. Pb concentration in the peat ranged from 2.18 to 68.33 mg kg^{-1}, while the atmospheric Pb deposition flux ranged from 0.12 to 12.49 mg m^{-2} a^{-1}. The Little Ice Age (cold and wet climate) led to low Pb concentration, Pb/Sc ratio, and Pb deposition flux (4.40 ± 0.70 mg kg^{-1}, 2.04 ± 0.38, and 0.28 ± 0.09 mg m^{-2} a^{-1}, respectively). On the other hand, intense volcanic eruptions resulted in high Pb concentration, Pb/Sc ratio, and P flux (54.48 ± 13.08 mg kg^{-1}, 7.85 ± 2.09, and 8.15 ± 2.85 mg m^{-2} a^{-1}, respectively). In addition, rapid economic development since the 1980s resulted in a gradual increase of anthropogenic Pb concentration from 1.54 mg kg^{-1} to 5.85 mg kg^{-1}; thus, the anthropogenic Pb deposition flux (0.43 ± 0.21 mg m^{-2} a^{-1}) was high during this period. In general, peat Pb concentration and atmospheric Pb deposition fluxes in this region have been affected by climate change, volcanic eruptions, and human activities. It was further demonstrated that atmospheric Pb emissions and deposition in China decreased since leaded gasoline was phased out in 2001. The results are critical to understand the geochemistry of Pb and to assess the effects of human activities on atmospheric Pb emissions and deposition in China.
© 2019 Elsevier Ltd. All rights reserved.

1. Introduction

Environmental pollution by toxic metals is a long-standing problem. Since the discovery of ancient mining and metal-working techniques, there have been close links between metals, metal pollution, and human activity (Nriagu, 1996). Both atmospheric and environmental pollution by toxic metals has been extensively investigated via retrospective geochemical monitoring using ombrotrophic peatlands as natural archives (Martínez-Cortizas et al., 1999; Shotyk et al., 1998). Ombrotrophic peatlands receive their nutrients and pollutants solely from the atmosphere and consequently enable the reconstruction of absolute atmospheric deposition rates (Shotyk, 1996a). During the past three decades, changes in the concentrations of heavy metals revealed by ombrotrophic peatland profiles have been widely used to reconstruct reliable pollution histories, mainly in Europe and Canada (Martínez-Cortizas et al., 1999; Pratte et al., 2013; Rausch et al., 2005; Shotyk et al., 1998, 2017).

Human activities, climate change, and volcanic eruptions all impact the atmospheric Pb deposition flux (Martínez-Cortizas et al.,

* Corresponding author.
E-mail address: c.lin@bnu.edu.cn (C. Lin).

https://doi.org/10.1016/j.chemosphere.2019.04.047
0045-6535/© 2019 Elsevier Ltd. All rights reserved.

1999; Shotyk, 1996a; 1998). Previous studies have shown that Pb is effectively immobile in ombrotrophic peatlands, which therefore accurately preserve atmospheric Pb deposition trends. Thus, Pb has received considerable attention, with many previous studies reporting independent records of atmospheric Pb deposition using peat cores (De Vleeschouwer et al., 2007; Ferrat et al., 2012; Kempter et al., 1997; Markert and Thornton, 1990; Martínez-Cortizas et al., 2002; Pratte et al., 2013, 2018; Shotyk, 1996a, 1996b; Shotyk et al., 1998, 2016a; 2016b; Vile et al., 1995).

Although ombrotrophic peatlands are widely distributed in northeast China and the Qinghai-Tibet plateau, areas that are famous for environmental pollution by toxic metals from coal and fuel burning and metal smelting in recent decades (Li et al., 2012; Shao et al., 2013), historical atmospheric metal pollution and deposition using ombrotrophic peat cores as natural archives has only received minimal research attention (Ferrat et al., 2012; Pratte et al., 2018. Until now, the longest time series of atmospheric Pb deposition history in China was conducted by Ferrat et al. (2012) using a 620-cm peat core from an ombrotrophic peatland in the eastern Qinghai-Tibet Plateau, which revealed an average atmospheric Pb deposition flux of 0.22 ± 0.24 mg m^{-2} a^{-1} over the last 9.5 ka. In addition, the Pb deposition flux was low (0.16 ± 0.08 mg m^{-2} a^{-1}) from 900 BP to approximately 300 BP.

Long-term environmental records of atmospheric Pb deposition in China, specifically northeast China, are relatively sparse. The Changbai Mountains in northeast China have experienced several significant climate shifts between dry and warm and wet and cold periods in the past 6000 years (Hong et al., 2001). The Changbai Volcano has a history of violent explosive Holocene activity, including one of the largest explosive eruptions on Earth in the last 2000 years (Machida and Arai, 1983; Wei et al., 2003). Northeast China is an old and traditional industrial base with abundant natural resources and many resource-based cities. Heavy metal emissions have increased in parallel with rapid industrialization and urbanization during the late 20th and 21st centuries (Li et al., 2012; Shao et al., 2013). How human activities, climate change, and volcanic eruptions affect atmospheric Pb deposition flux in northeast China is not clear, but critical to understand the regional geochemistry of Pb. Ombrotrophic peat cores in the Changbai Mountains might represent a valuable study area for investigating the effects of climate change, volcanic eruptions, and human activities on atmospheric Pb deposition in northeast China.

The main objectives of this study are to produce a concentration profile for Pb in a peat core measuring 320 cm depth collected from an ombrotrophic peatland in the Changbai Mountains, estimate long-term anthropogenic and lithogenic fluxes of atmospheric Pb deposition, and identify the effect of human activities, climate change, and volcanic eruption on atmospheric Pb deposition in this region.

2. Materials and methods

2.1. Site description

The Jinchuan peatland (42°22′N, 126°26′E) is located in the Changbai Mountains in northeast China, with an area of 0.85 km^2, an average peat accumulation thickness of 4–5 m, and an elevation of 700 m a.s.l. (Jiang et al., 2008; Mao et al., 2002). The peatland originates from a maar formed by volcanic activity of the Longgang Volcano group and exhibits relatively stable hydrological conditions (Hong et al., 2000). The region is characterized by an East Asian monsoon climate of warm and humid weather in the summer and cold and dry weather in the winter. The average annual temperature and precipitation are 3 °C and 700 mm, respectively. Approximately 150 km to the east of the study area, the Changbai Volcano and the peak of the Changbai Mountains lie on the border of China and Korea (2691 m a.s.l., the highest peak on the Chinese side) (Jiang et al., 2008). The present-day vegetation is bryophytes (*Sphagnum subsecundum*, *S. palustre*, *S. capillifolium*, and *S. fallax*) and vascular plants (*Carex limosa*, *C. lasiocarpa*, *Oxycoccus palustris*, *Parathelypteris glanduligera*, *C. leucochlora*, *Phragmites australis*, *Viola Verecunda*, *Sanguisorba parviflora, etc.*) (Zeng et al., 2012).

2.2. Peat core collection

Two peat cores were collected from the same site using a percussion drilling set (product code: 04.19.SC, Eijkelkamp, Netherlands) with a core sampler equipped with a PVC sample tube (100 cm long and 4.5 cm inner diameter). The geographic coordinates of the peat site are 42.35061°N and 126.37242°E with an altitude of 622 m. The peat cores were brought back to the laboratory, cut into 1-cm slices, and freeze-dried. Although the peat profile depth was 320 cm, the obtained peat core was only 164 cm due to the compression effect. Therefore, 1-cm slices represent an actual average thickness of 1.95 (320/164 = 1.95) cm. The actual depth for each slice was calculated assuming that the peat cores were evenly compressed. Previous studies on the era of volcano eruptions and the depth of volcanic eruption-derived materials in the peat profile have verified that this assumption is generally reasonable (see explanation in 3.1 section) (Machida et al., 1990; Mao et al., 2002). The bulk density calculated using the actual thickness and dry weight of each slice ranged from 25.1 mg cm^{-3} to 131.1 mg cm^{-3}, with an average of 75.0 mg cm^{-3} (Table 1), which is generally similar to that of a peatland profile in the eastern Qinghai–Tibetan Plateau (3–831 mg cm^{-3} with an average of 86 mg cm^{-3}) (Large et al., 2009). The peat samples from one peat core were used for dating, while those from the other core were used for ash and elemental analysis.

2.3. Sample analyses

Approximately 0.5 g peat samples were dried at 105 °C for 12 h and ashed in a furnace at 450 °C for a further 12 h. The ash content was determined as a percentage of the dry weight for each peat sample (Ferrat et al., 2012). Then, the ash was completely transferred to a 50-mL Teflon beaker and digested with HNO_3-HF-$HClO_4$ (Lin et al., 2008). All reagents were of analytical grade. The concentrations of Sc and Pb were measured using ICP-MS (X Series II, Thermo Electron), while the concentrations of Al, Ti, Ca, Mg, and Sr were determined using ICP-OES (IRIS Intrepid II, Thermo Electron).

Together with digestion and measurement of the peat ash samples, four reference materials were digested and analyzed four times to check the analytical quality. Note that peat samples were

Table 1
Basic statistical parameters of bulk density, ash content, and elemental concentrations in peat core samples (n = 164).

	Unit	Mean	Median	SD	CV%	Max	Min
Bulk Density	mg/cm^3	73.18	72.91	18.75	25.6	138.71	25.16
Ash	%	23.12	22.90	6.99	30.2	48.31	8.77
Pb	mg/kg	9.00	6.27	10.41	115.6	68.33	2.18
Sc	mg/kg	3.28	2.84	1.53	46.6	8.10	0.82
Sr	mg/kg	73.18	70.25	20.08	27.4	124.91	29.49
Ti	mg/kg	1128	952	558	49.5	3551	296
Al_2O_3	%	2.95	2.37	1.64	55.7	8.51	0.82
Fe_2O_3	%	1.31	1.15	0.62	46.9	4.02	0.45
MgO	%	0.34	0.30	0.15	43.8	0.88	0.12
CaO	%	0.75	0.71	0.18	23.8	1.36	0.31
Na_2O	%	0.30	0.25	0.19	63.1	1.00	0.05
K_2O	%	0.49	0.42	0.26	53.8	1.40	0.15

Table 2
Comparison of Pb concentration and flux for the peat core at Jinchuan site of Changbai Mountains, northeast China with those for other peat cores in China and around world.

Country	Site	Core depth	Pb Concentration	Pb Flux	Reference
		cm	mg kg^{-1}	mg m^{-2} yr^{-1}	
China	Jichuan (Changbai Mts.)	320	2.2–20.2[a]	0.12–3.9[a]	This study
China	Hongyuan (Tibet Pleatau)	620	2.9–21.6	0.06–3.5	Ferrat et al. (2012)
Switzerland	Etang de la Gruere	650	0.2–85.5	0.01–15.7	Shotyk et al. (1998)
	Etang de la Gruere	36	14.7–85.5	2.0–15.5	Weiss et al. (1999b)
	Praz Rodez	60	8.9–64.0	6.6–12.5	
	Schopfenwaldmoor	25	29.1–69.7	1.8–8.5	
	La Tourbiere des Genevez	39	15.8–43.0	6.9–15.3	
	Gola di Lago	33	76.8–1527.8	15–277	
Western Scotland	Loch Laxford	80	1.6–35.8		Weiss et al. (2002)
Scotland	Flanders Moss	106	1–264	0.8–21	Cloy et al. (2005)
Sweden	Store Mosse	568	0.1–14.2		Kylander et al. (2013)
Cezch	Ore Mts., Jizerske Mts, Sumava	40	46–392	12.2–40	Zuna et al. (2011)
Belgium	Misten Bog	680	12.3–949		De Vleeschouwer et al. (2007)
Russia	West Siberia	280	0.2–7.0	0.1–0.5	Veretennikova (2015)
Spain	Peda da Cadela	185	1–84	0.01–5.7	Martinez Cortizas et al., 2002
	Penido Vello	250	1–87	0.02–7.3	
Canada	North Alberta	65	0.3–11.5	0.1–2.3	Shotyk et al. (2016b)
Eastern Canada	Point Escuminac	80	0.9–52.5		Weiss et al. (2002)
Canada	St. Lawrence	100	0.5–320	0.03–47	Pratte et al. (2013)

[a] Excluding the data for volcanic eruption period.

ashed before digestion and various types of soil were used as reference materials (GSS13: loamy soil from Huabei Plain; GSS15: clayey soil from middle-lower Changjiang River Plain; GSS17: sandy soil from Inner Mongolia; GSS25: loess from Shaanxi Loess Plain). The average relative errors ranged from 4.41% for Pb to −0.25% for Ti (n = 16). The precision of the methods was assessed by replicate analyses of 11 peat samples. The average coefficients of variance (CV) for the replicate analyses ranged from 6.70% for Sc to 3.21% for Ca. Detailed data of the relative errors and CV are shown in Appendix Tables 1 and 2.

2.4. Dating

The ^{210}Pb and ^{137}Cs dating of the samples from 0 to 85 cm depth was conducted and analyzed at the Radionuclide Dating Laboratory, Institute of Geology and Geophysics, Chinese Academy of Sciences, using a Canberra well-detector gamma spectrometer (GCW3023) and constant activity model (Sanchez-Cabeza and Ruiz-Fernandez, 2012) (Appendix Table 3). The small peak of ^{137}Cs activity was identified at 10.8 cm depth, which likely corresponds to the peak ^{137}Cs fallout in 1963 AD. However, the decreasing trend of ^{137}Cs activity with depth might be due to its diffusion and advection through pore water as well as biological uptake by vegetation (Mihalík et al., 2014; Turetsky et al., 2004). ^{14}C dating and analysis of 10 peat samples below a depth of 50 cm was conducted at the Accelerator Mass Spectrometry and Quaternary Dating Laboratory of Peking University by radiocarbon accelerator mass spectrometry. All original ^{14}C ages were calibrated to calendar years using IntCal04 (Reimer et al., 2004) (Appendix Table 4). The half-lives are 22.23 a for ^{210}Pb and 5568 a for ^{14}C, and the ^{210}Pb dating method is suitable for measuring several tens of years BP, while the ^{14}C dating method is suitable for the measurement of thousands of years BP. Therefore, the ^{210}Pb age data from 0 to 30 cm depth and ^{14}C age data from 80 to 320 cm depth were used to construct the depth-age relationship using the BACON model (Appendix Fig. 1). Previous studies on the depth of volcanic eruption-derived materials in the peat profile and the age of volcano eruptions have further validated the constructed depth-age relationship (see explanation in 3.1 section) (Machida et al., 1990; Mao et al., 2002).

2.5. Calculation of atmospheric Pb deposition flux

The conservative element Sc is often used to quantify anthropogenic Pb in soils and sediments (Ferrat et al., 2012; Lin et al., 2008; Shotyk, 1996b; Shotyk et al., 1998, 2016c; Weiss et al., 1999a). The anthropogenic Pb concentration ($[Pb]_A$) in each peat sample was calculated as follows:

$$[Pb]_L = [Sc]_M \left([Pb]/[Sc]\right)_{background} \quad [1]$$

$$[Pb]_A = [Pb]_M - [Pb]_L \quad [2]$$

where $[Pb]_L$ is the lithogenic Pb concentration; $[Pb]_M$ and $[Sc]_M$ are the measured concentrations in the peat sample; and $([Pb]/[Sc])_{background}$ is the natural background Pb/Sc ratio. In this study, the average Pb/Sc ratio (1.81) in the upper crust (Taylor and McLennan, 1995) was used as the natural background Pb/Sc ratio to differentiate the anthropogenic Pb from lithogenic Pb. If the calculated $[Pb]_L$ was higher than the measured $[Pb]_M$ for several layers, then $[Pb]_L$ was assumed to be equal to $[Pb]_M$.

The atmospheric Pb deposition flux ($Pb_{slice\ flux}$, mg m^{-2} a^{-1}) for each slice was calculated as follows:

$$Pb_{slice\ flux} = \frac{C_i \times m_i \times 10^{-3}}{s \times \Delta t_i} \quad [3]$$

where C_i is the Pb concentration (mg/kg) in slice i; m_i is the peat sample mass (g) for slice i; s is the cross-sectional area of the peat core (m^2); and Δt_i is the formation time for slice i (a).

3. Results and discussion

3.1. Geochemical indicators of peatland trophic status

Geochemical indicators, such as ash, Al, Ti, Ca, Mg, and Sr contents, have often been used to constrain the trophic status of peat cores (Weiss et al., 1999a). Ash, Al_2O_3, CaO, MgO, Ti, and Sr contents in Jinchuan peatland (Table 1, Fig. 1) were similar to those for other peatlands in the Changbai Mountains and Qinghai-Tibet Plateau (Bao et al., 2010; Ferrat et al., 2012; Jia et al., 2006; Zhao et al.,

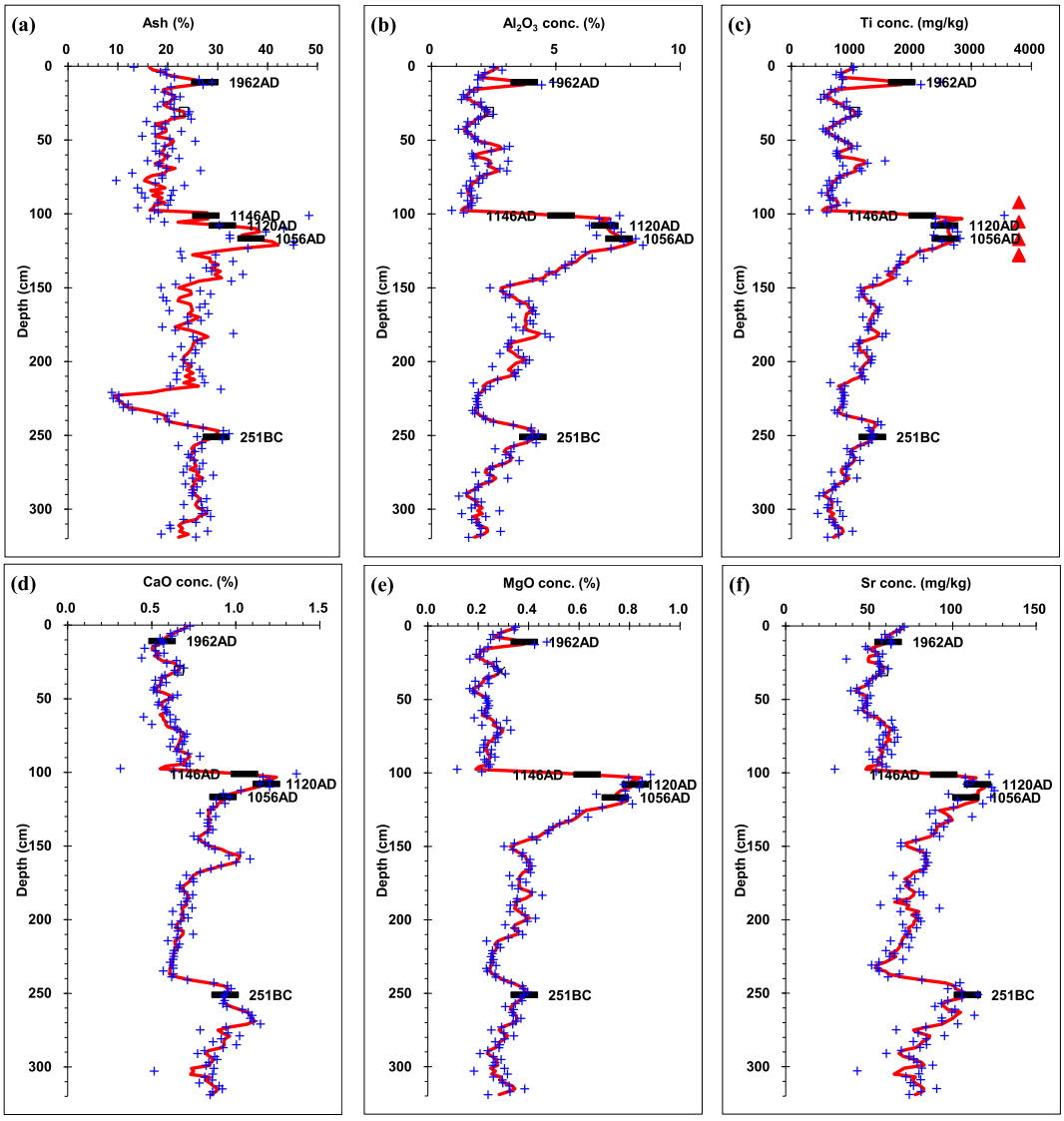

Fig. 1. Changes in ash, Al_2O_3, Ti, CaO, MgO, and Sr contents in the peat core with profile depth. The individual points represent measured values and the curves are smoothed by a 3-point moving average. Recorded ages (triangles) of volcanic eruptions of the Changbai Volcano are shown in panel (c) (Wei et al., 2003).

2004). The concentration profiles of the elements were characterized by high peak at 100–120 cm depth and moderate high peaks at 250–256 cm depth and 10-cm depth. The concentration peaks of these elements and ash at 100–120 cm depth are related to intense volcanic eruptions that occurred around the 11th century from Changbai Volcano, which led to extensive ash fall in and around the Sea of Japan (Machida and Arai, 1983; Machida et al., 1990). The concentration peaks of elements and ash at 250–260 cm depth might be related to volcanic eruptions of the Longgang Volcano group, as indicated by Mao et al. (2002), who found volcanic glass at 252–255 cm depth in the Jinchuan peat profile and attributed it to *in-situ* deposition of Longgang volcanic material. Moreover, large-scale deforestation for farming occurred in northeast China in the 1950s–1960s, which might have increased atmospheric dust deposition and generated the slightly high ash, Al, Mg, and Ti contents in the peat at approximately 10-cm depth.

As expected, the A1 profile generally resembled the distribution of ash (Fig. 1). Ti exhibited conservative behavior in weathering environments, and also followed the general distribution of ash. In addition, the Al content was significantly correlated with the Ti content, with a correlation coefficient of 0.921 (Appendix Fig. 2). The profiles of ash, Al, and Ti typically imply that inorganic material contents in the peat were supplied by soil dust rather than sediment dissolution (Ferrat et al., 2012; Kylander et al., 2005; Martínez-Cortizas et al., 2002). The Ca/Mg molar ratio of the peats relative to the corresponding ratio in rainwater is one way of distinguishing between ombrotrophic peats and minerotrophic peats (Shotyk, 1996a). At the Longfengshan background station (44°44′N, 127°36′E, 331 a.s.l.) nearest to the Jinchuan peatland, the Ca/Mg molar ratio in rainwater was approximately 4.1 from 1991 to 1997 (Yang et al., 2002), while the ratio was 3.6 and 3.4 in 2006 and 2007, respectively (Li et al., 2010). Therefore, the Ca/Mg molar ratio in the peat was lower than that of the average rainwater composition, showing that the peat core is ombrotrophic (Appendix Fig. 3). In other words, the inorganic constituents in the peat core were supplied exclusively by atmospheric deposition. In general, an increase in Sr content with peat profile depth can indicate groundwater movement by the vertical migration of this element (Ferrat et al., 2012). For the Jinchuan peat, Sr showed no increase with depth (Appendix Fig. 2), further suggesting that the metal elements

in the peat bog were supplied by soil dust rather than sediment dissolution.

In summary, the vertical distributions of ash, Al, Ti, Ca, Mg, and Sr contents in the peat profile and the Ca/Mg molar ratio in the peat samples generally suggest that the peat core at Jinchuan is ombrotrophic and hence can be used as a natural archive to reconstruct the history of atmospheric Pb deposition.

3.2. Concentration profiles of lead and scandium

Pb concentration ranged from 2.18 mg kg^{-1} at 98 cm depth (1167 AD) to 68.33 mg kg^{-1} at 106 cm depth (1120 AD). Sc concentration varied between 0.82 mg kg^{-1} at 98 cm depth (1167 AD) and 8.10 mg kg^{-1} at 117 cm depth (1056 AD) (Table 1, Fig. 2). High Pb concentration (29.65–68.33 mg kg^{-1}) was observed in the layers between 101 cm depth (1146 AD) and 114 cm depth (1069 AD). The average concentration of Pb in the remaining layers was 6.97 ± 3.10 mg kg^{-1} (n = 157). This average value was similar to the Pb concentration (6.80 ± 4.18 mg kg^{-1}, n = 63) in the ombrotrophic peat archives of the eastern Qinghai-Tibet Plateau (Ferrat et al., 2012). This result indicates similar Pb concentration in the atmospheric deposits of these two areas. We identified five periods according to the changes of Pb and Sc concentrations and Pb/Sc ratio along the peat profile.

3.2.1. Period I (dry and warm climate)

From 320 cm depth (1681 BC) to 115 cm depth (1062 AD), Pb and Sc concentrations generally displayed a gradually increasing trend, while the Pb/Sc ratio was generally constant with an average of 2.31 ± 0.35 (n = 97) (Fig. 2). This value is similar to that in the upper continental crust (17/7 = 2.43) reported by Wedepohl (1995) but higher than that in the upper continental crust (20/11 = 1.82)

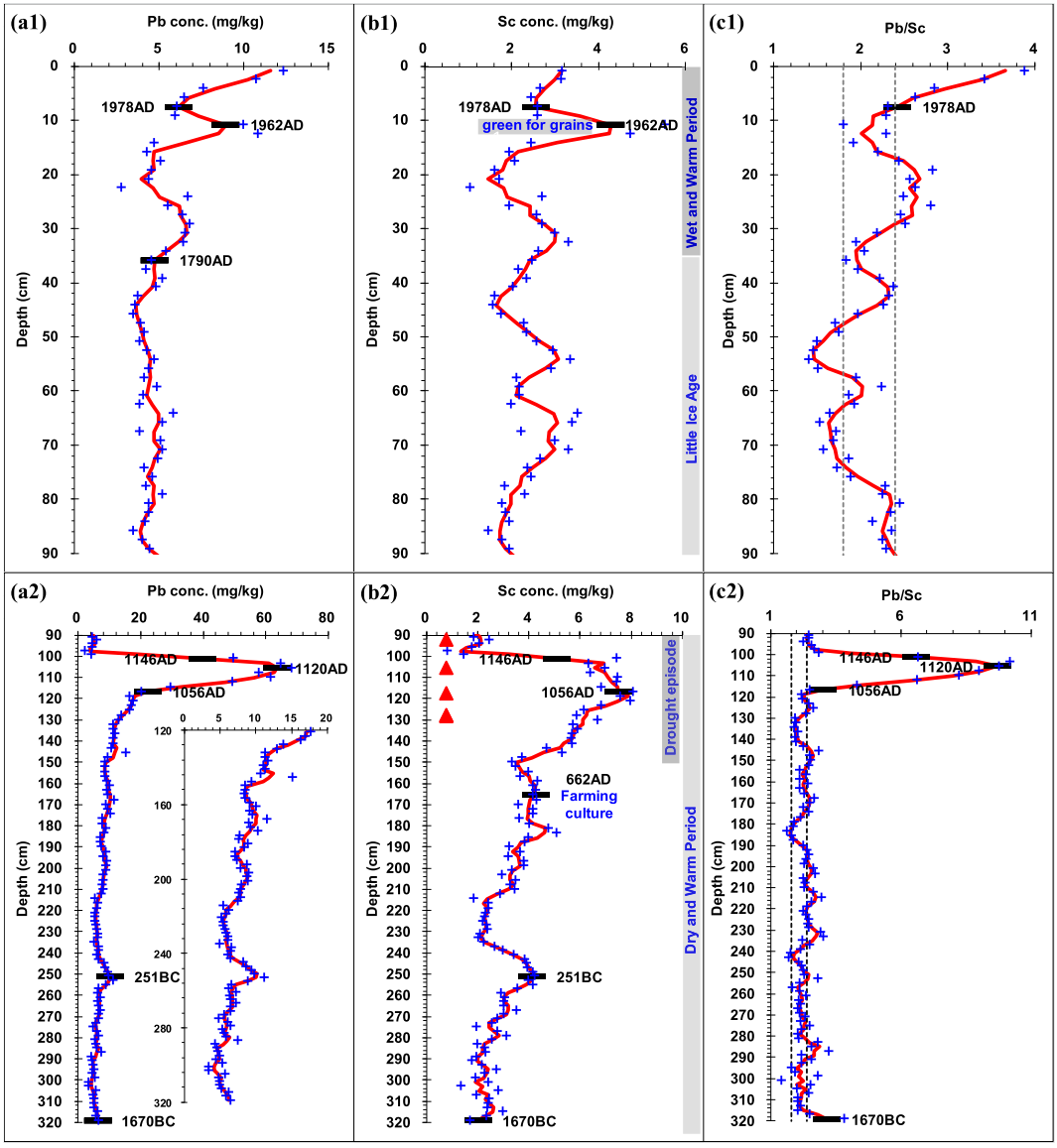

Fig. 2. Changes in Pb (a) and Sc (b) contents and Pb/Sc ratio (c) in the peat core with profile depth. (a1) to (c1) show 0–90 cm depth in the peat core, while (a2) to (c2) show 90–320 cm depth. The individual points represent measured values and the curves are smoothed using a 3-point moving average. Recorded ages (triangles) of volcanic eruptions of the Changbai Volcano are shown in panel (b) (Wei et al., 2003) as well as climate change (Hong et al., 2001). The two vertical dotted lines in panel (c) represent the values for Pb/Sc in the upper continental crust (Taylor and McLennan, 1995; Wedepohl, 1995).

reported by Taylor and McLennan (1995). In addition, Pb concentration was significantly correlated to Sc concentration ($R^2 = 0.864$, $n = 97$) in this period (Appendix Fig. 2). These results suggest that most of the Pb content in each layer is supplied by lithogenic atmospheric soil dust. The gradually increasing trends of Pb and Sc concentrations might be related to climate change because four drought episodes occurred at approximately 50–150 AD, 250–400 AD, 600–750 AD, and 820–1200 AD (Hong et al., 2001).

3.2.2. Period II (eruption of the Changbai Volcano)

From 115 cm depth (1062 AD) to 100 cm depth (1152 AD), high Pb concentration led to the highest Pb/Sc ratio (4.33–10.21) (Fig. 2). The high Pb concentration and Pb/Sc ratio are assumed to be related to intense eruptions of the Changbai Volcano in approximately the 11th century (Machida and Arai, 1983). Zhang et al. (2015) investigated the elemental compositions of volcanic rocks from the Changbai Volcano eruption and reported a Pb/Sc ratio in pumice from 4.6 to 9.8. This further demonstrates that the high Pb concentration peaks are related to the largest-scale intense volcanic activity of the Changbai Volcano. In addition, the steep peaks of Pb concentration and Pb/Sc that correspond with intense volcanic eruptions further suggests that atmospheric Pb deposition can be recorded by the peat bogs of the Changbai Mountains in northeast China.

3.2.3. Period III (the Little Ice Age)

From 100 cm depth (1152 AD) to 35 cm depth (1800 AD), the Pb concentration and Pb/Sc ratio averaged 4.40 ± 0.71 mg kg^{-1} and 2.04 ± 0.38 ($n = 39$), respectively, which are lower than those (8.08 ± 3.19 for Pb and 2.31 ± 0.35 for Pb/Sc) for 320–115 cm depth (Fig. 2). The climate was relatively wet and cold during the Little Ice Age (from approximately the 1200s AD to 1800s AD) (Hong et al., 2001). The average Pb/Sc ratio in the period is similar to that (1.82) in the upper continental crust reported by Taylor and McLennan (1995) but lower than that in the upper continental crust (2.43) reported by Wedepohl, 1995). Therefore, the Pb/Sc ratio (1.82) in the upper continental crust was used to differentiate the anthropogenic Pb from lithogenic Pb in the peatland profile in this study.

3.2.4. Period IV and V (warm and wet climate)

The climate became relatively wet and warm after the 1800s AD (Hong et al., 2001). This period was arbitrarily divided into two subperiods according to Pb concentration and Pb/Sc ratio: period V from 1974 AD to 2013 AD (8.3 cm depth to surface) and period IV from 1800 AD to 1974 AD (35–8.3 cm depth). For period IV, Pb concentration and Pb/Sc ratio averaged 6.03 ± 2.00 (2.79–10.85) mg kg^{-1} and 2.34 ± 0.31 (1.81–2.83) ($n = 16$), respectively. A previous study indicated that Pb concentration was higher than 20 mg kg^{-1} and Pb/Sc ratio was greater than 150 in the EGr (Etang de la Gruyère) peat core in Switzerland from 1905 AD to 1979 AD (Shotyk et al., 1998), showing that anthropogenic Pb deposition was higher in central Europe than in northeast China during this period. For period V above 8.3 cm depth (since 1974 AD), Pb concentration gradually increased from 6.05 to 12.36 mg kg^{-1} and Pb/Sc ratio increased from 2.32 to 3.89 (Fig. 2). These results indicate that the effect of human activities on atmospheric Pb deposition has increased in northeast China since the economic reforms of China. In contrast, Pb concentration has rapidly decreased in the EGr peat core in Switzerland since approximately 1979 (Shotyk et al., 1998).

3.3. Flux of atmospheric lead deposition

The change of atmospheric Pb deposition flux is shown in Fig. 3. It is characterized by an overall gradual increase since 1800 AD and a high peak band for the Changbai Volcano eruption period from 1062 AD to 1152 AD.

Total atmospheric Pb deposition flux generally increased from 0.23 mg m^{-2} a^{-1} at 37.5 cm depth (1771 AD) to 0.99 mg m^{-2} a^{-1} at the surface (2010 AD), with peaks at 10.8 cm and 2.5 cm. For the Little Ice Age period from 92 cm depth (1200 AD) to 35 cm depth (1800 AD), the total atmospheric deposition flux was low, with an average of 0.28 ± 0.09 ($n = 34$) mg m^{-2} a^{-1}. The large-scale intense eruption of the Changbai Volcano in approximately the 11th century led to high total atmospheric Pb deposition flux from 115 cm to 100 cm depth, with average and maximum values of 8.15 ± 2.85 ($n = 7$) and 12.49 mg m^{-2} a^{-1}, respectively. Before this volcanic eruption, the total atmospheric Pb deposition flux was characterized into three gradually increasing intervals, which were likely due to an increasingly dry climate with drought episodes. A previous study indicated that the average base flux of total atmospheric Pb deposition was 0.22 ± 0.24 mg m^{-2} a^{-1} in an ombrotrophic peat core on the Qinghai-Tibet Plateau (Ferrat et al., 2012). This value is in a similar range to that of our study for the Little Ice Age period. In addition, the Pb concentration range for the peat core from the Qinghai-Tibet Plateau is also similar to our result excluding the intense volcanic eruption period (Table 2).

As the effect of human activities on atmospheric Pb deposition has been dominant over the last several hundred years, the anthropogenic atmospheric Pb deposition flux was estimated since 1200 AD. From 1200 AD to 1800 AD (the Little Ice Age period), the anthropogenic atmospheric deposition flux was low, with an average of 0.03 ± 0.03 ($n = 34$) mg m^{-2} a^{-1}. However, the anthropogenic atmospheric Pb deposition flux typically increased from 0.03 mg m^{-2} a^{-1} in 1800 AD to 0.24 mg m^{-2} a^{-1} in 1927 AD. This increase might be ascribed to the early industrialization of China. It was estimated that global anthropgenic emissions of Pb to atmosphere increased from about 100 metirc tons in 1850 to 1100 metric tons in 1930 (Nriagu, 1996). From 1927 AD to 1978 AD, the anthropogenic atmospheric Pb deposition flux varied from 0.11 to 0.30 mg m^{-2} a^{-1}, which might be related to wars and cultural revolution (slow development of economy) in China. Subsequently, the anthropogenic atmospheric Pb deposition flux rapidly increased from 0.25 mg m^{-2} a^{-1} in 1987 AD to 0.74 mg m^{-2} a^{-1} in 2003 AD due to rapid economic development of China after economic reform. The decrease of the anthropogenic atmospheric Pb deposition flux from 2003 to 2010 could be ascribed to the decline of leaded gasoline, economic recession in northeast China, and greater clean production. Leaded gasoline was officially phased out in 2001, thus atmospheric Pb emissions quickly dropped (Li et al., 2012). A previous study showed that the average anthropogenic Pb emission flux in the past 30 years in Jilin Province was 0.82 mg m^{-2} a^{-1} (Li et al., 2012). Pb emitted into the atmosphere mostly falls in the areas around emission sources (Lei et al., 2016); thus, the anthropogenic atmospheric Pb deposition flux recorded in ombrotrophic peatlands far from emission sources is assumed to be less than the anthropogenic atmospheric Pb emission flux recorded in Jilin Province.

In general, Pb concentration and flux in/from the peat core at Jinchuan site, Changbai Mountains were similar to those at Honghuan (Tibet Plateau, China), north Alberta (Canada), and Pena da Cadela and Penido Vello (Xistral Mountains, Spain) (Ferrat et al., 2012; Martinze Cortizas et al., 2002; Shotyk et al., 2016b), but lower than those at some sites of some European countries and Canada (Cloy et al., 2005; De Vleeschouwer et al., 2007; Kylander et al., 2013; Pratte et al., 2013; Shotyk et al., 1998; Weiss et al., 1999b, 2002; Zuna et al., 2011). However, Pb concentration and flux in/from the peat core of Great Vasyugan Mire in West Siberia, Russia was the lowest (Veretennikova, 2015).

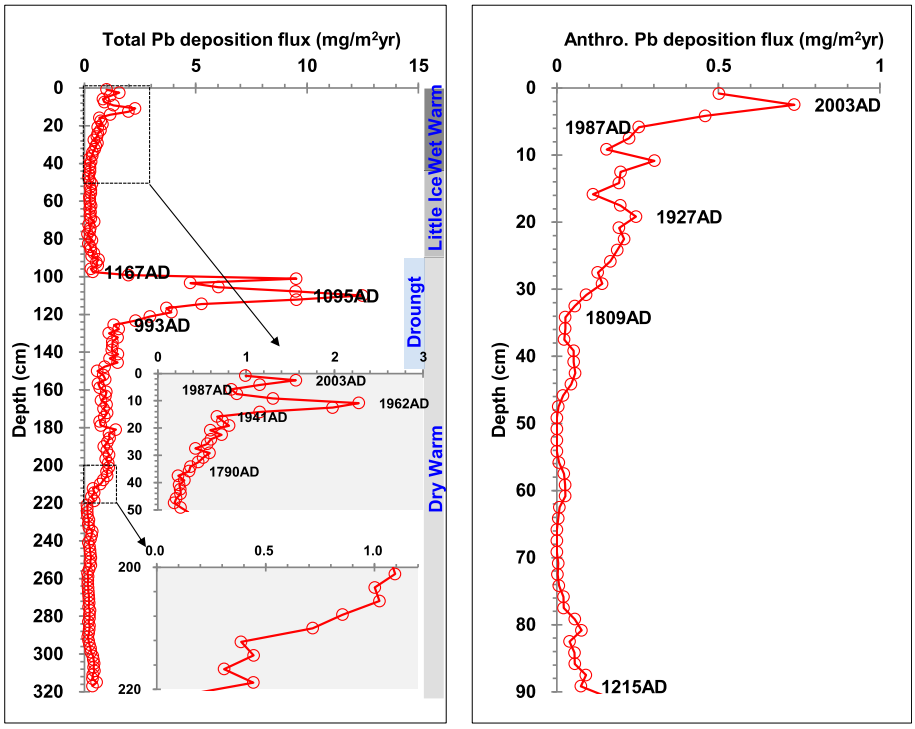

Fig. 3. Total and anthropogenic atmospheric Pb deposition flux for each slice (depth) of the peat profile.

4. Conclusions

The long-term fluxes of atmospheric Pb deposition are critical to understand the geochemistry of Pb and to assess the effects of human activities on atmospheric Pb emissions and deposition. Using an ombrotrophic peat core from the Changbai Mountains, we firstly assessed the Pb concentration and atmospheric Pb deposition flux in the past 3600 years for northeast China. Pb concentration in the whole peat core averaged 9.00 ± 6.27 (2.18–68.33, n = 164) mg kg^{-1}, whereas the Pb/Sc ratio was 2.5 ± 1.3 (1.4–10.2, n = 164). The average baselines for Pb concentration and Pb/Sc ratio were 4.40 ± 0.70 mg kg^{-1} and 2.04 ± 0.38 (n = 39), respectively, and the baseline for Pb flux was 0.28 mg m^{-2} a^{-1}, derived from the Little Ice Age period. Extensive volcanic eruptions led to a substantial increase in Pb concentration, Pb/Sc ratio, and Pb flux for the period of 1062 AD to 1152 AD, with values of 29.65–68.33 mg kg^{-1}, 4.33 to 10.21, and 4.76–12.49 mg m^{-2} a^{-1}, respectively. Rapid economic development since the 1980s resulted in the gradual increase of anthropogenic Pb concentration from 1.54 mg kg^{-1} in the 1980s to 5.85 mg kg^{-1} in the 2010s. The average total, lithogenic, and anthropogenic Pb fluxes were 1.09, 0.65, and 0.44 mg m^{-2} a^{-1} for the past 40 years, respectively. It was found that Pb concentration and flux were generally higher for dry and warm climate periods than for wet and cold climate periods. Extensive volcanic eruptions greatly increased Pb concentration and flux. Rapid economic development over the last 40 years increased the anthropogenic Pb concentration and flux in northeast China. This study further demonstrated that atmospheric Pb emissions and deposition in China decreased since leaded gasoline was phased out in 2001.

Acknowledgements

This work was supported by the National Natural Science Foundation of China (U1706217, 41671462, 41171359) and the Fundamental Research Funds for the Central Universities (No. 2017XTCX02).

Appendix

Table 1
Measured concentrations and relative errors of Pb and other elements in reference soils (GSS13: loamy soil from Huabei Plain; GSS15: clayey soil from middle-lower Changjiang River Plain; GSS17: sandy soil from Inner Mongolia; GSS25: loess from Shaanxi Loess Plain).

		Reference value	Measured value	Measured value	Measured value	Measured value	Average error
Reference material GSS13: Loamy soil from Huabei Plain							
Pb	mg/kg	21.60	22.10	24.14	24.44	23.28	8.75%
Sc	mg/kg	10.50	10.73	10.85	10.77	11.16	3.60%
Sr	mg/kg	195.0	203.2	210.8	205.9	186.3	3.36%
Ti	mg/kg	3820	3496	4040	3578	3863	−1.98%
Al_2O_3	%	11.76	11.75	12.49	11.83	11.66	1.47%
Fe_2O_3	%	4.11	4.01	4.14	4.02	4.23	−0.25%
MgO	%	2.05	2.10	2.15	2.04	2.07	1.87%

(*continued on next page*)

Table 1 (*continued*)

		Reference value	Measured value	Measured value	Measured value	Measured value	Average error
CaO	%	5.00	5.04	5.32	5.09	5.10	2.75%
Reference material GSS15: Clayey soil from middle-lower Changjiang River Plain							
Pb	mg/kg	38.00	39.27	39.69	43.05	42.04	7.93%
Sc	mg/kg	14.80	15.66	15.75	16.54	16.32	8.56%
Sr	mg/kg	115.0	130.2	118.7	126.5	126.5	9.10%
Ti	mg/kg	5270	5161	4684	5673	5498	−0.30%
Al_2O_3	%	15.27	15.44	15.90	16.15	15.95	3.86%
Fe_2O_3	%	6.44	6.12	6.22	6.53	6.55	−1.27%
MgO	%	1.80	1.74	1.80	1.85	1.81	0.01%
CaO	%	1.53	1.53	1.62	1.66	1.67	5.90%
Reference material GSS17: Sandy soil from Inner Mongolia							
Pb	mg/kg	17.40	17.16	18.42	18.41	17.10	2.14%
Sc	mg/kg	5.10	4.80	5.21	5.13	4.78	−2.39%
Sr	mg/kg	209.0	203.1	219.3	221.7	208.5	1.99%
Ti	mg/kg	1910	1837	2108	2074	1954	4.35%
Al_2O_3	%	9.65	9.01	10.01	9.83	9.28	−1.24%
Fe_2O_3	%	2.07	2.14	2.11	2.17	2.07	2.52%
MgO	%	0.78	0.74	0.82	0.81	0.78	1.27%
CaO	%	1.83	1.73	1.89	1.89	1.82	0.07%
Reference material GSS25: Loess from Shaanxi Loess Plain							
Pb	mg/kg	22.00	20.21	21.67	22.12		−3.04%
Sc	mg/kg	11.60	10.67	11.56	11.45		−3.18%
Sr	mg/kg	192.0	182.9	192.1	208.5		1.30%
Ti	mg/kg	3900	3624	3800	3804		−4.03%
Al_2O_3	%	11.76	11.16	11.69	12.33		−0.27%
Fe_2O_3	%	4.30	4.10	4.14	4.28		−2.96%
MgO	%	1.99	1.82	1.98	1.96		−3.40%
CaO	%	7.18	7.05	7.29	7.28		0.39%

Table 2
Duplicate measurement and average CV (coefficient of variance) of Pb and other element concentrations for 11 peat samples.

		Pb mg/kg	Sc mg/kg	Sr mg/kg	Ti mg/kg	Al_2O_3 %	MgO %	CaO %
Sample 1	Replica 1	6.88	2.82	55.06	924	2.02	0.29	0.67
	Replica 2	6.59	2.58	58.11	922	1.97	0.26	0.63
Sample 2	Replica 1	4.13	2.40	50.48	767	1.57	0.22	0.62
	Replica 2	4.14	2.32	47.74	794	1.91	0.24	0.64
Sample 3	Replica 1	4.06	2.18	58.65	751	1.82	0.27	0.70
	Replica 2	4.18	2.57	58.58	856	2.06	0.28	0.71
Sample 4	Replica 1	3.89	1.21	57.62	566	1.25	0.21	0.63
	Replica 2	4.45	1.29	50.93	613	1.34	0.22	0.63
Sample 5	Replica 1	11.28	5.73	95.33	1873	5.80	0.58	0.85
	Replica 2	11.39	5.75	99.63	1747	5.49	0.54	0.83
Sample 6	Replica 1	9.20	3.70	83.00	1349	3.80	0.38	0.79
	Replica 2	10.05	4.17	82.03	1542	4.34	0.42	0.91
Smaple 7	Replica 1	8.78	3.60	77.44	1256	3.80	0.43	0.71
	Replica 2	8.81	3.99	81.93	1419	4.09	0.42	0.73
Sample 8	Replica 1	6.41	2.23	54.07	866	1.98	0.27	0.64
	Replica 2	5.97	1.99	48.86	842	1.80	0.27	0.61
Sample 9	Replica 1	7.23	2.78	90.07	1001	3.20	0.33	0.99
	Replica 2	7.25	3.36	94.45	1049	3.21	0.35	1.08
Sample 10	Replica 1	4.90	1.78	67.99	499	1.24	0.22	0.79
	Replica 2	4.33	1.78	62.60	429	1.14	0.19	0.76
Sample 11	Replica 1	6.71	1.57	68.88	570	1.46	0.21	0.85
	Replica 2	6.33	1.83	79.33	635	1.54	0.22	0.85
Average CV		3.63%	6.67%	4.62%	5.82%	5.88%	4.45%	3.21%

Table 3
Radioactivity of ^{226}Ra, ^{210}Pb, and ^{137}Cs and estimated age by ^{226}Ra and ^{210}Pb using constant flux model (also called as constant rate of supply model) for the 0–83 cm depth of the peat core.

Sample	^{226}Ra		^{210}Pb		^{137}Cs		$^{210}Pb_{ex}$	^{210}Pb Age	
depth	mean	±δ	mean	±δ	mean	±δ	Bq/kg	yrs BP	
cm	Bq/kg	Bq/kg	Bq/kg	Bq/kg	Bq/kg	Bq/kg			
0.83	11.50	0.83	721.17	12.50	101.00	1.50	709.67	−63.49	2013 AD
4.17	11.67	0.83	611.33	11.83	90.67	1.50	599.67	−49.73	2000 AD
7.50	12.33	0.83	360.33	11.17	11.83	0.75	348.00	−29.96	1980 AD
10.83	13.83	0.83	158.17	11.33	19.00	0.83	144.33	−12.03	1962 AD
14.17	15.00	0.67	101.33	8.17	9.83	0.50	86.33	0.18	1950 AD
17.50	10.67	1.00	93.67	14.33	8.33	0.83	83.00	10.46	1940 AD
20.83	11.33	0.83	89.50	12.50	5.33	0.50	78.17	21.50	1929 AD
24.17	11.50	1.00	43.50	8.33	3.17	0.50	32.00	30.50	1919 AD
27.50	11.50	0.83	35.33	9.00	0.17	0.17	23.83	37.38	1913 AD
30.83	9.33	0.83	28.67	8.33	–		19.33	44.98	1905 AD
34.17	9.17	0.83	27.83	8.00	–		18.67	52.37	1898 AD
37.50	10.17	1.00	45.67	8.50	–		35.50	63.19	1887 AD
40.83	11.00	1.00	38.83	8.67	–		27.83	89.79	1860 AD
44.17	11.50	1.00	15.67	7.83	–		4.17		
47.50	12.50	0.83	8.17	7.33	–		−4.33		
50.83	12.17	0.83	3.50	6.83	–		−8.67		
54.17	11.67	0.83	14.83	7.33	–		3.17		
57.50	11.50	1.00	15.00	8.33	–		3.50		
60.83	10.00	1.00	11.67	9.83	–		1.67		
64.17	9.67	1.00	7.50	6.33	–		−2.17		
67.50	13.50	1.17	15.33	11.33	–		1.83		
70.83	12.67	1.17	8.50	10.33	–		−4.17		
74.17	11.83	1.17	8.00	11.50	–		−3.83		
77.50	11.67	1.17	14.50	10.67	–		2.83		
80.83	11.67	1.17	8.33	9.83	–		−3.33		

$^{210}Pb_{ex}$: Excess ^{210}Pb = ^{210}Pb radioactivity − ^{226}Ra radioactivity.
–: Radioactivity is below detection limit.
Notes: Whereas the peat of ^{137}Cs radioactivity at 10.83 cm depth is small, it might still correspond to 1963, the year of peak ^{137}Cs fallout. In addition, ^{210}Pb dated era is 1962 at this depth, which is similar to that dated by ^{137}Cs. Therefore, ^{210}Pb dating data are generally reasonable for the top 30 cm depth of the core.

Table 4
^{14}C age and calibrated ^{14}C date by OxCall v3.10 program using IntCal04 curve for the peat core.

Sample	^{14}C age		Calibrated ^{14}C date	
depth	mean	±δ	68.2% probability	95.4% probability
cm	BP	BP		
2.59	Modern carbon			
50.86	655	20	1285 AD (29.8%) 1305 AD 1360 AD (38.4%) 1385 AD	1280 AD (44.1%) 1320 AD 1350 AD (51.3%) 1390 AD
85.34	820	35	1185 AD (5.6%) 1200 AD 1205 AD (62.6%) 1265 AD	1160 AD (95.4%) 1280 AD
118.75	965	30	1020 AD (25.4%) 1050 AD 1080 AD (42.8%) 1150 AD	1010 AD (95.4%) 1160 AD
148.75	1210	30	775 AD (68.2%) 875 AD	690 AD (12.2%) 750 AD 760 AD (83.2%) 900 AD
175.75	1480	30	555 AD (68.2%) 615 AD	530 AD (95.4%) 650 AD
207.25	1515	35	460 AD (7.0%) 490 AD 530 AD (62.1%) 610 AD	430 AD (95.4%) 620 AD
238.38	1680	40	260 AD (6.4%) 280 AD 330 AD (61.8%) 420 AD	240 AD (95.4%) 440 AD
266.32	2665	30	835 BC (68.2%) 795 BC	900 BC (95.4%) 790 BC
3215		35	1515 BC (68.2%) 1440 BC	1610 BC (4.3%) 1570 BC 1540 BC (91.1%) 1410 BC
317.79	3340	35	1690 BC (53.4%) 1600 BC 1580 BC (14.8%) 1530 BC	1740 BC (3.6%) 1710 BC 1700 BC (91.8%) 1520 BC

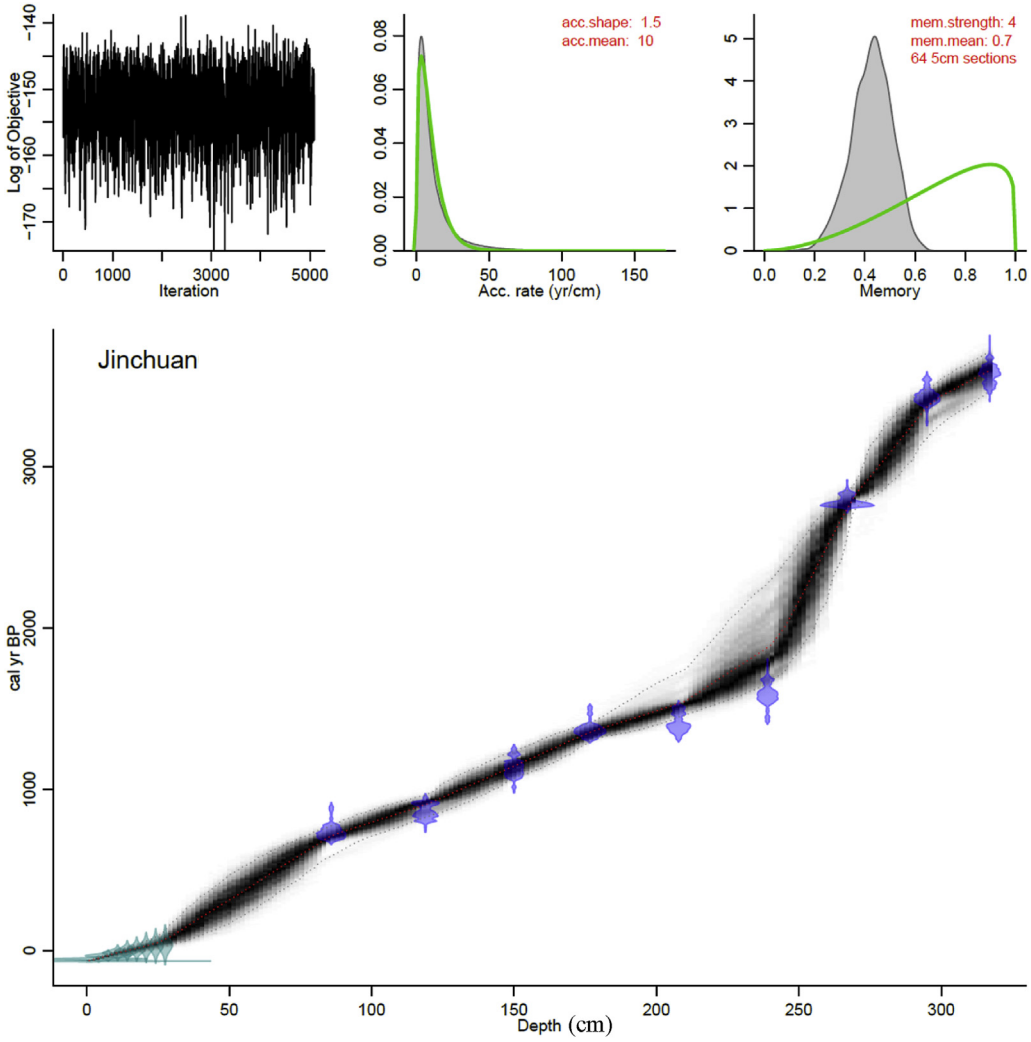

Fig. 1. Simulated relationship between calibrated yrs BP (1950) and depth by Bacon Model using ^{210}Pb age data for the 0–30 cm depth of the peat core and ^{14}C age data for the 80–320 cm depth of the peat core. The simulated weighted average age data are used in this paper.

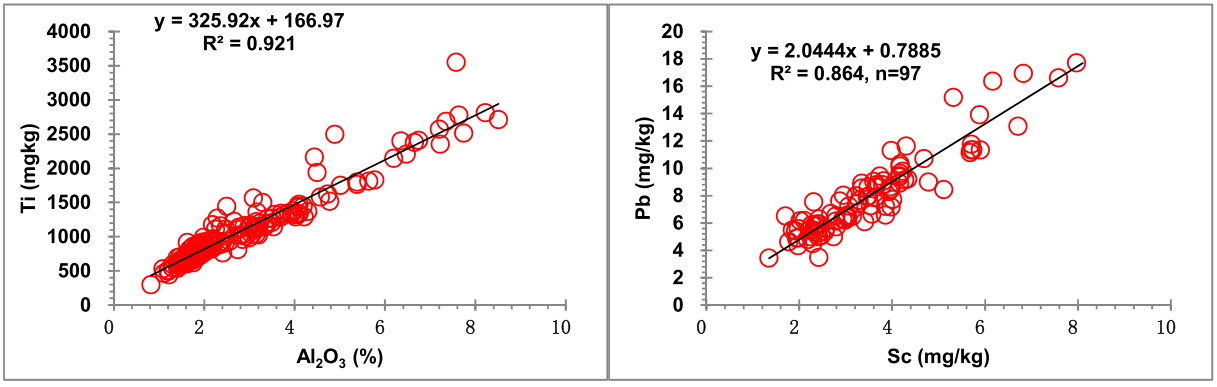

Fig. 2. Concentrations relationships of Al ~ Ti and Pb ~ Sc in the peat core samples at Jichuan site, Changbain Mountains.

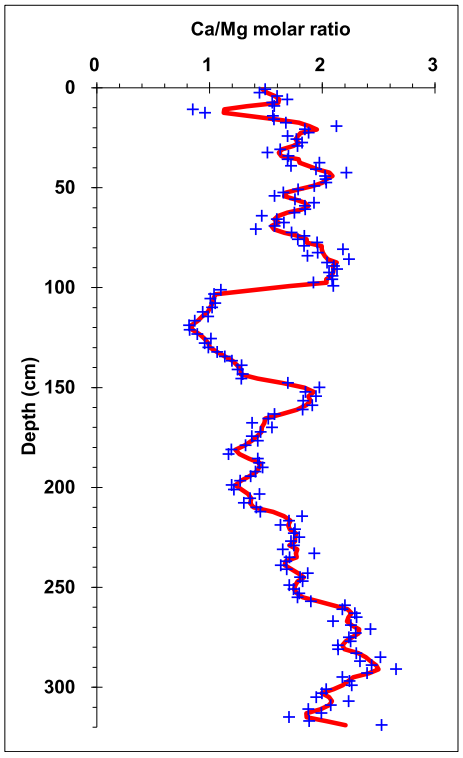

Fig. 3. Molar ratio Ca/Mg in the peat profile. The average Ca/Mg molar ratio in rainwater in the adjacent part (44°44′N, 127°36′E, 331 a.s.l.) was 4.10 from 1991 to 1997 (n = 134).

References

Bao, K.S., Yu, X.F., Jia, L., Wang, G.P., 2010. Recent carbon accumulation in Changbai mountain peatlands, northeast China. Mt. Res. Dev. 30, 33–41.

Cloy, J.M., Farmer, J.G., Graham, M.C., MacKenzie, A.B., Cook, G.T., 2005. A comparison of antimony and lead profiles over the past 2500 years in Flanders Moss ombrotrophic peat bog, Scotland. J. Environ. Monit. 7, 1137–1147.

De Vleeschouwer, F., Gérard, L., Goormaghtigh, C., Mattielli, N., Le Roux, G., Fagel, N., 2007. Atmospheric lead and heavy metal pollution records from a Belgian peat bog spanning the last two millenia: human impact on a regional to global scale. Sci. Total Environ. 377, 282–295.

Ferrat, M., Weiss, D.J., Dong, S.F., Large, D.J., Spiro, B., Sun, Y.B., Gallagher, K., 2012. Lead atmospheric deposition rates and isotopic trends in Asian dust during the last 9.5 kyr recorded in an ombrotrophic peat bog on the eastern Qinghai–Tibetan Plateau. Geochem. Cosmochim. Acta 82, 4–22.

Hong, Y.T., Jiang, H.B., Liu, T.S., Zhou, L.P., Beer, J., Li, H.D., Leng, X.T., Hong, B., Qin, X.G., 2000. Response of climate to solar forcing recorded in a 6000-year $\delta^{18}O$ time-series of Chinese peat cellulose. Holocene 10, 1–7.

Hong, Y.T., Wang, Z.G., Jiang, H.B., Lin, Q.H., Hong, B., Zhu, Y.X., Wang, Y., Xu, L.S., Leng, X.T., Li, H.D., 2001. A 6000-year record of changes in drought and precipitation in northeastern China based on a N13C time series from peat cellulose. Earth Planet. Sci. Lett. 185, 111–119.

Jia, L., Wang, G.P., Liu, J.S., 2006. Distribution and implication of major and trace elements in peat profiles of Yuanchi, Changbai Mountain. J. Mountain Sci. 24, 662–666 (in Chinese with English abstract).

Jiang, W.Y., Leroy, A.G.S., Ogle, N., Chu, G.Q., Wang, L., Li, J.Q., 2008. Natural and anthropogenic forest fires recorded in the Holocene pollen record from a Jinchuan peat bog, northeastern China. Palaeogeogr. Palaeoecol. 261, 47–57.

Kempter, H., Gorres, M., Frenzel, B., 1997. Ti and Pb concentrations in rainwater-fed bogs in Europe as indicators of past anthropogenic activities. Water Air Soil Pollut. 100, 367–377.

Kylander, M.E., Bindler, R., Martinez Cortizas, A., Gallagher, K., Morth, C.M., Rauch, S., 2013. A novel geochemical approach to paleorecords of dust deposition and effective humidity: 8500 years of peat accumulation at Store Mosse (the "Great Bog"), Sweden. Quat. Sci. Rev. 69, 69–82.

Kylander, M.E., Weiss, D.J., Martínze-Cortizas, A., Spiro, B., Garcia-Sanchez, R., Coles, B.J., 2005. Refining the pre-industrial atmospheric Pb isotope evolution curve in Europe using an 8000 year old peat core from NW Spain. Earth Planet. Sci. Lett. 240, 467–485.

Large, D.J., Spiro, B., Ferrat, M., Shopland, M., Kylander, M., Gallagher, K., Li, X.D., Shen, C.D., Possnert, G., Zhang, G., Darling, W.G., Weiss, D., 2009. The influence of climate, hydrology and permafrost on Holocene peat accumulation at 3500 m on the eastern Qinghai–Tibetan Plateau. Quat. Sci. Rev. 28, 3303–3314.

Lei, K., Giubilato, E., Critto, A., Pan, H.Y., Lin, C.Y., 2016. Contamination and human health risk of lead in soils around lead/zinc smelting areas in China. Environ. Sci. Pollut. Res. 23, 13128–13136.

Li, Q., Cheng, H.G., Zhou, T., Lin, C.Y., Guo, S., 2012. The estimated atmospheric lead emissions in China, 1990-2009. Atmos. Environ. 60, 1–8.

Li, Y., Yu, X.L., Cheng, H.B., Lin, W.L., Tang, J., Wang, S.F., 2010. Chemical characteristics of precipitation at three Chinese regional background stations from 2006 to 2007. Atmos. Res. 96, 173–183.

Lin, C.Y., He, M.C., Zhou, Y.X., Guo, W., Yang, Z.F., 2008. Distribution and contamination assessment of heavy metals in sediment of the Second Songhua River, China. Environ. Monit. Assess. 137, 329–342.

Machida, H., Arai, F., 1983. Extensive ash falls in and around the sea of Japan from large late quaternary eruptions. J. Volcanol. Geotherm. Res. 18, 151–164.

Machida, H., Moriwaki, H., Zhao, D., 1990. The recent major eruption of Changbai Volcano and its environmental effects. Geogr. Rep. Tokyo Metrop. Univ. 25, 1–20.

Mao, X.M., Hong, Y.T., Zhu, Y.X., Wang, H., 2002. Discovery of volcanic explosion-derived materials in Jinchuan peat and its significance. Acta Mineral. Sin. 22, 9–14 (in Chinese with English abstract).

Markert, B., Thornton, I., 1990. Multi-element analysis of an English peat bog soil. Water Air Soil Pollut. 49, 113–123.

Martínez-Cortizas, A., García-Rodeja, E., Pontevedra-Pombal, X., Nóvoa Muñoz, J.C., Weiss, D., Cheburkin, A., 2002. Atmospheric Pb deposition in Spain during the last 4600 years recorded by two ombrotrophic peat bogs and implications for the use of peat as archive. Sci. Total Environ. 292, 33–44.

Martínez-Cortizas, A., Pontevedra-Pombal, X., García-Rodeja, E., Nóva-Muñoz, J.C., Shotyk, W., 1999. Mercury in a Spanish peat bog: archive of climate change and atmospheric metal deposition. Science 284, 939-342.

Mihalík, H., Bartusková, M., Hölgye, Z., Ježková, T., Henych, O., 2014. Fractionation of ^{137}Cs Cand Pu in natural peatland. J. Environ. Radioact. 134, 14–20.

Nriagu, J.O., 1996. A history of global metal pollution. Science 272, 223–224.

Pratte, S., Bao, K.S., Shen, J., Mackenzie, L., Klamt, A.M., Wang, G.P., Xing, W., 2018. Recent atmospheric metal deposition in peatlands of northeast China: a review. Sci. Total Environ. 626, 1284–1294.

Pratte, S., Mucci, A., Garneau, M., 2013. Historical records of atmospheric metal deposition along the St. Lawrence Valley (eastern Canada) based on peat bog cores. Atmos. Environ. 79, 831–840.

Rausch, N., Nieminen, T., Ukonmaanaho, L., Le Roux, G., Krachler, M., Cheburkin, A.K., Bonani, G., Shotyk, W., 2005. Comparison of atmospheric deposition of copper, nickel, cobalt, zinc, and cadmium recorded by Finnish peat cores with monitoring data and emission records. Environ. Sci. Technol. 39, 5989–5998.

Reimer, P.J., Baillie, M.G.L., Bard, E., Bayliss, A., Beck, J.W., Bertrand, C.J.H., et al., 2004. IntCal04 terrestrial radiocarbon age calibration, 26-0 ka BP. Radiocarbon 46, 1029–1058.

Sanchez-Cabeza, J.A., Ruiz-Fernandez, A.C., 2012. ^{210}Pb sediment radiochronology: an integrated formulation and classification of dating models. Geochem. Cosmochim. Acta 82, 183–200.

Shao, X., Cheng, H.G., Li, Q., Lin, C.Y., 2013. Anthropogenic atmospheric emissions of cadmium in China. Atmos. Environ. 75, 155–160.

Shotyk, W., 1996a. Peat bog archives of atmospheric metal deposition: geochemical evaluation of peat profile, natural variations in metal concentrations, and metal enrichment factors. Environ. Rev. 4, 149–183.

Shotyk, W., 1996b. Natural and anthropogenic enrichments of As, Cu, Pb, Sb, and Zn in ombrotrophic versus minerotrophic peat bog profiles, Jura Mountains, Switzerland. Water Air Soil Pollut. 90, 375–405.

Shotyk, W., Appleby, P.G., Bicalho, B., Davies, L., Froese, D., Grant-Weaver, I., Krachler, M., Magnan, G., Mullan-Boudreau, G., Noernberg, T., Pelletier, R., Shannon, B., van Bellen, S., Zaccone, C., 2016b. Peat bogs in northern Alberta, Canada reveal decades of declining atmospheric Pb contamination. Geophys. Res. Lett. 43, 9964–9974.

Shotyk, W., Appleby, P.G., Bicalho, B., Davies, L.J., Froese, D., Grant-Weaver, I., Magnan, G., Mullan-Boudreau, G., Noernbery, T., Pelletier, R., Shannon, B., van Bellen, S., Zaccone, C., 2017. Peat bogs document decades of declining atmospheric contamination by trace metals in the Athabasca Bituminous Sands Region. Environ. Sci. Technol. 51, 6237–6249.

Shotyk, W., Bicalho, B., Cuss, C.W., Duke, M.J.M., Noernberg, T., Pelletier, R., Zaccone, C., 2016c. Dust is the dominant source of "heavy metals" to peat moss (Sphagnum fuscum) in the bogs of the Athabasca Bituminous Sands region of northern Alberta. Environ. Int. 92–93, 494–506.

Shotyk, W., Rausch, N., Outridge, P.M., Krachler, M., 2016a. Isotopic evolution of atmospheric Pb from metallurgical processing in Flin Flon, Manitoba: retrospective analysis using peat cores from bogs. Environ. Pollut. 218, 338–348.

Shotyk, W., Weiss, D., Appleby, P.G., Cheburkin, A.K., Frei, R., Gloor, M., Kramers, J.D., Reese, S., Van der Knaap, W.O., 1998. History of atmospheric lead deposition since 12,370 14C yr BP from a peat bog, Jura Mountains, Switzerland. Science 281, 1635–1640.

Taylor, S.R., McLennan, S.M., 1995. The geochemical evolution of the continental crust. Rev. Geophys. 33, 241–265.

Turetsky, M.R., Manning, S.W., Wieder, R.K., 2004. Dating recent peat deposits. Wetlands 24, 324–356.

Veretennikova, E.E., 2015. Lead in the natural peat cores of ridge-hollow complex in the taiga zone of West Siberia. Ecol. Eng. 80, 100–107.

Vile, M.A., Novak, M.J.V., Brizova, E., Wieder, R.K., Schell, W.R., 1995. Historical rates of atmospheric Pb deposition using ^{210}Pb dated peat cores: corroboration, computation, and interpretation. Water Air Soil Pollut. 79, 89–106.

Wedepohl, K.H., 1995. The composition of the continental crust. Geochem. Cosmochim. Acta 59, 1217–1232.

Wei, H., Sparks, R.S.J., Liu, R., Fan, Q., Wang, Y., Hong, H., Zhang, H., Chen, H., Jiang, C., Dong, J., Zheng, Y., Pan, Y., 2003. Three active volcanoes in China and their hazards. J. Asian Earth Sci. 21, 515–526.

Weiss, D., Shotyk, W., Appleby, P.G., Kramers, J.D., Cheburkin, A.K., 1999b. Atmospheric Pb deposition since the industrial revolution recorded by five Swiss peat profiles: enrichment factors, fluxes, isotopic composition, and sources. Environ. Sci. Technol. 33, 1340–1352.

Weiss, D., Shotyk, W., Boyle, E.A., Kramers, J.D., Appleby, P.G., Cheburkin, A.K., 2002. Comparative study of the temporal evolution of atmospheric lead deposition in Scotland and eastern Canada using blanket peat bogs. Sci. Total Environ. 292, 7–18.

Weiss, D., Shotyk, W., Kempf, O., 1999a. Archives of atmospheric lead pollution. Naturwissenschaften 86, 262–275.

Yang, D.Z., Zhou, H.G., Zhang, Z.H., 2002. Chemical characteristics of precipitation in regional air pollution background stations of China. J. Applied Meteorological Sci. 13 (4), 430–439 (in Chinese with English abstract).

Zeng, J., Bu, Z.J., Ma, J.Z., Zhao, G.L., Long, C., Li, W., Zhang, B.J., Qu, H., Feng, L., 2012. Interspecific correlations among bryophytes and among bryophytes and vascular plants in two scales in Jinchuan Peatland. Plant Sci. J. 30, 459–467 (in Chinese with English abstract).

Zhang, M.L., Guo, Z.F., Cheng, Z.H., Zhang, L.H., Liu, J.Q., 2015. Late Cenozoic intraplate volcanism in Changbai volcanic field, on the border of China and North Korea: insights into deep subduction of the Pacific slab and intraplate volcanism. J. Geol. Soc. London 172, 648–663.

Zhao, H.Y., Wang, S.Z., Li, H.K., 2004. Geochemistry of the Holocene peatland in Changbaishan Mountains and its implication for paleoenvironmental change. J. Palaeogeogr. 6 (3), 355–362 (in Chinese with English abstract).

Zuna, M., Mihaljevic, M., Sebek, O., Ettler, V., Handley, M., Navratil, T., Golias, V., 2011. Recent lead deposition trends in the Czech Republic as recorded by peat bogs and tree rings. Atmos. Environ. 45, 4950–4958.